SENFTLEBEN-BEENAKKER EFFECTS IN DIFFUSING AND HEAT CONDUCTING GAS MIXTURES

H.F.P. Knaap, G.W. 't Hooft, E. Mazur and L.J.F. Hermans
Huygens Laboratorium, Rijksuniversiteit Leiden, The Netherlands

ABSTRACT

The influence of an external field on the transport phenomena in polyatomic gases leads to detailed information about the kinetic theory of such gases. In particular, a magnetic field gives rise to transverse transport, perpendicular to both the macroscopic gradient and the field. The present experimental results, along with other recent results from our laboratory, comprise a complete set of data on such transverse effects occurring in heat conducting and diffusing gas mixtures, *viz.*, simple heat conduction and diffusion and also their cross effects, thermal diffusion and the diffusion-thermo effect. Special emphasis is given to the phenomenology of these effects and to experimental techniques.

I. INTRODUCTION

Experimental studies on the influence of magnetic and electric fields on gas transport properties (the so-called *Senftleben-Beenakker effects*) have now progressed so far, that a survey of results on these effects is in order. Theoretical studies have proven that these data provide essential information concerning the binary interaction of polyatomic molecules. Why an external field influences the transport properties of polyatomic gases and how this effect is related to the nonspherical part of the molecular interaction potential can be understood in the following way. By applying a macroscopic gradient in a polyatomic gas, not only an anisotropy in the velocity distribution is produced, but via collisions also anisotropies (*polarizations*) in the combined velocity and angular momentum space. The collisional production of these anisotropies is strongly determined by the angle dependent part of the intermolecular potential. If now a magnetic field is applied the field will interact with the

---

Presented as invited extended contribution 60 at the 11th International Symposium on Rarefied Gas Dynamics, Cannes, July 3-8, 1978.

This work is part of the research program of the "Stichting voor Fundamenteel Onderzoek der Materie (FOM)" and has been made possible by financial support from the "Nederlandse Organisatie voor Zuiver-Wetenschappelijk Onderzoek (ZWO)".

magnetic moments that the molecules possess due to their rotation

$$\underline{\mu} = g \frac{\underline{J}}{\hbar} \mu_N \qquad (1)$$

where g is the molecular g-factor, $\underline{J}$ the rotational angular momentum and μ_N the nuclear magneton. The resulting Larmor-precession of the angular momenta around the field direction will partially destroy the anisotropy in the velocity-angular momentum space. This will cause the transport properties to change. The typical condition for this effect to occur, is expressed by $\omega\tau \approx 1$, where ω is the Larmor precession frequency proportional to the field strength B and τ is the time scale for the decay of an angular momentum dependent polarization through collisions, which is inversely proportional to the pressure p. Hence field effects are expected to be functions of B/p. For molecules having electric dipole moments, precession can also be achieved by applying an electric field E; in that case the effects are generally functions of E/p.

The field dependences of the effects are - for a given polyatomic gas - different for each angular momentum dependent polarization present. Hence measurements of the change in transport properties will give information on the relative importance of the various angular momentum dependent polarizations, which are, as already mentioned, determined by the nonspherical part of the molecular interaction potential.

For *dilute* polyatomic gases these field effects on transport properties have been studied extensively over the last years (some references to experimental work can be found in Table I). For various kinds of molecules experiments have been carried out for the magnetic field influence on the shear viscosity η and the thermal conductivity λ. The effect was studied as a function of temperature both in pure polyatomic gases and in mixtures with noble gases. Similar experiments have been performed in an electric field. In addition field effects on the thermal diffusion and its reciprocal effect, the diffusion-thermo effect or Dufour effect, have been studied in various polyatomic-noble gas mixtures. Finally the magnetic field effect on diffusion was measured most recently. It should also be mentioned that measurements of the field effects on transport phenomena of *rarefied* polyatomic gases (*1/p effects*) have also been performed (see, *e.g.*, contributed paper 59).

Table I

Some references to experimental work on magnetic and electric field effects in dilute polyatomic gases

Magnetic field effects on		Ref.	Remarks
Shear viscosity	η	1,2,3,4,5	pure gases/mixtures/ various temperatures
Thermal conductivity	λ	6,7,8,9,10,11	pure gases/mixtures/ various temperatures
Thermal diffusion	D_T	12,13	mixtures/T = 300 K
Dufour effect	$\mathscr{D}_T$	14,15	N_2-Ar (.50-.50)/ T^2= 300 K
Diffusion	D	16	mixtures/T = 300 K
Electric field effects on		**Ref.**	**Remarks**
Shear viscosity	η	17,18,19	
Thermal conductivity	λ	18,20,21,22	
Thermal diffusion	D_T	23	

II. THEORY

In this paper we will restrict ourselves to the magnetic field effects in heat conducting and diffusing gases. As illustration of these magnetic field effects we will first discuss heat conduction through a polyatomic gas in a magnetic field. In the presence of a magnetic field the thermal conductivity λ is no longer isotropic. Using symmetry arguments it can be shown, that the energy flux density is then described phenomenologically by the generalized Fourier law

$$\underline{q} = -\lambda.\underline{\nabla}T \quad . \tag{2a}$$

When the magnetic field $\underline{B}$ is taken into the z-direction, $\underline{B}$ = (0, 0, B), the second rank tensor $\underline{\underline{\lambda}}$ is of the form

$$\underline{\underline{\lambda}} = \begin{pmatrix} \lambda^{\perp} & -\lambda^{tr} & 0 \\ \lambda^{tr} & \lambda^{\perp} & 0 \\ 0 & 0 & \lambda^{//} \end{pmatrix} . \qquad (2b)$$

The physical meaning of the three coefficients $\lambda^{//}$, $\lambda^{\perp}$ and λ^{tr} is shown in Fig. 1. The diagonal elements denote the heat flow

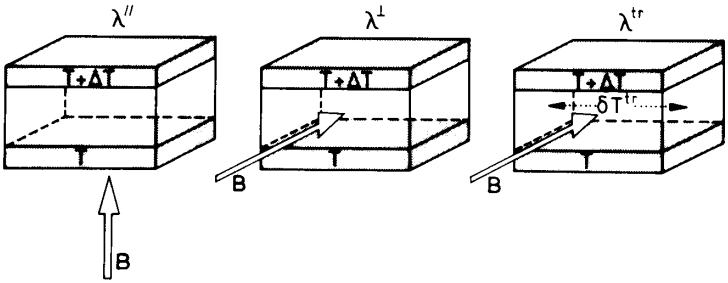

Fig. 1. The physical meaning of the thermal conductivity coefficients $\lambda^{//}$, $\lambda^{\perp}$ and λ^{tr} in a magnetic field $\underline{B}$. Note that in the absence of the field, $\lambda^{//} = \lambda^{\perp} = \lambda(0)$ and $\lambda^{tr} = 0$.

parallel to an applied temperature gradient in the presence of a magnetic field parallel to the gradient ($\lambda^{//}$) or perpendicular to the gradient ($\lambda^{\perp}$), while λ^{tr} corresponds to transverse heat flow perpendicular to both applied temperature gradient and magnetic field. The quantities $\lambda^{//}$ and $\lambda^{\perp}$ are analogous to magnetoresistance in electrical conductance, while λ^{tr} is analogous to the Hall coefficient. As in the electrical analogon $\lambda^{//}$ and $\lambda^{\perp}$ are even functions of the field, while λ^{tr} is an odd function of the field. Experimentally one finds indeed for polyatomic gases that the quantities $\Delta\lambda^{\perp} = \lambda^{\perp}(B) - \lambda(0)$ ($\lambda(0)$ is the field free thermal conductivity coefficient), $\Delta\lambda^{//} = \lambda^{//}(B) - \lambda(0)$ and λ^{tr} are nonzero.

A kinetic theory treatment for the various field effects has been developed. Although different methods and techniques for calculating field dependences and magnitudes of field effects exist, basically all methods start with a Chapman-Enskog type of perturbation theory: the one-particle distribution function f for a gas in the presence of a macroscopic gradient (*e.g.*, a temperature or concentration gradient) differs slightly from the Maxwellian equilibrium function $f^{(0)}$. The deviation is expressed as

$$f = f^{(0)} (1 + \phi) , \qquad (3)$$

ϕ being the deviation from equilibrium, linear in the first derivatives of temperature, concentration etc. (second order derivatives which lead to Burnett coefficients play a crucial role only in the rarefied gas regime and can be neglected in the dilute gas regime). Thus, in the case of a temperature gradient, *e.g.*, one has

$$\phi = -\underline{A}.\underline{\nabla}T \ . \tag{4}$$

For noble gases the vectorial quantity $\underline{A}$ is a vector function of the reduced molecular velocity $\underline{W}$. For a gas of polyatomic molecules, however, the situation is more complicated since then two vector quantities, namely the reduced molecular velocity $\underline{W}$ and the angular momentum $\underline{J}$, must be taken into account. Consequently $\underline{A}$ has to be expanded in terms of the polar vectors, which can be constructed from $\underline{W}$ and $\underline{J}$

$$\underline{A} = a_1\underline{W} + a_2\ (\underline{W}.\underline{J})\underline{J} + a_3\ (\underline{W} \wedge \underline{J}) \ . \tag{5}$$

The second and third terms in Eq. (5) are the angular momentum dependent polarizations, which give rise to the field effects. For a detailed theoretical treatment the reader is referred to Refs. 24-29. It was found that the field dependences of the elements of the transport tensor $\underline{\underline{\lambda}}$ have the following form[11,30,31,32]

$$\frac{\Delta\lambda^{/\!/}}{\lambda} = -\Psi^{\lambda}_{12}\left[\ 2f(\omega\tau_{12}) \qquad\qquad\ \right] + \Psi^{\lambda}_{11}\ 2f(\omega\tau_{12}) \tag{6}$$

$$\frac{\Delta\lambda^{\perp}}{\lambda} = -\Psi^{\lambda}_{12}\left[\ f(\omega\tau_{12}) + 2f(2\omega\tau_{12})\ \right] + \Psi^{\lambda}_{11}\ \ f(\omega\tau_{12}) \tag{7}$$

$$\frac{\lambda^{tr}}{\lambda} = -\Psi^{\lambda}_{12}\left[\ g(\omega\tau_{12}) + 2g(2\omega\tau_{12})\ \right] + \Psi^{\lambda}_{11}\ \ g(\omega\tau_{12}) \tag{8}$$

with

$$f(\omega\tau) = \frac{\omega^2\tau^2}{1 + \omega^2\tau^2} \tag{9}$$

and

$$g(\omega\tau) = \frac{\omega\tau}{1 + \omega^2\tau^2} \ . \tag{10}$$

Ψ^{λ}_{12} and Ψ^{λ}_{11} reflect the contributions of the $\underline{W}\ \underline{J}\ \underline{J}$ polarization (the second term in Eq. (5)) and the $\underline{W}\ \underline{J}$ polarization (the third term of Eq. (5)), respectively, while τ_{12} and τ_{11} are the time scales for the decay of the polarizations and ω is the

Larmor precession frequency

$$\omega = \frac{g\,\mu_N\,B}{\hbar} \,. \tag{11}$$

The quantities Ψ^{λ}_{12}, Ψ^{λ}_{11}, τ_{12} and τ_{11} can be determined by the experiment.

As an example results for N_2 are shown in Fig. 2. The experimental results could be fitted to the theoretical expressions (Eqs. (6), (7) and (8)) using Ψ^{λ}_{12}, Ψ^{λ}_{11}, τ_{12} and τ_{11} as

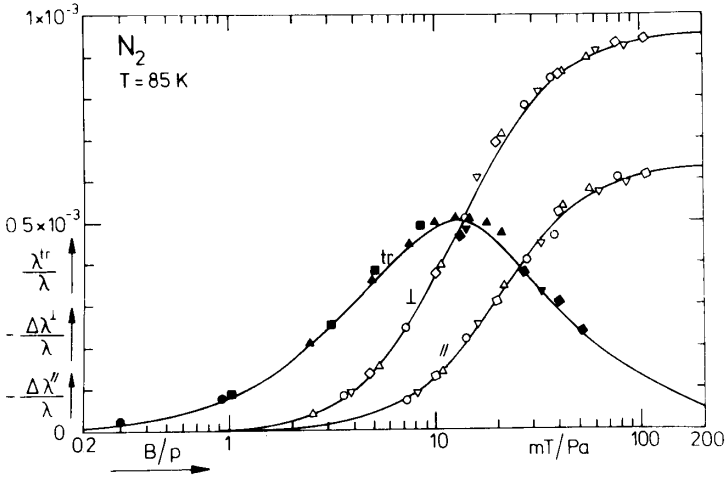

Fig. 2. Results for the three thermal conductivity coefficients for N_2. The curves drawn through the experimental points represent the theoretical expressions (Eqs. (6), (7) and (8)). The behavior as a function of B/p reflects the typical dominance of the W J J polarization (the second term in Eq. (5)) found for most simple gases.

adaptable parameters. It was found that the dominant contribution to the effects stems from the W J J polarization. For some gases also a small contribution from the W J polarization was found. The most sensitive method for evaluating the importance of the W J polarization is to study $(\Delta\lambda^{\perp}/\Delta\lambda^{/\!/})_{sat}$, the ratio of $\Delta\lambda^{\perp}/\lambda$ and $\Delta\lambda^{/\!/}/\lambda$ at high B/p values[8]. This ratio can be determined in *one* apparatus and is therefore not affected by systematic errors.

In the case of binary gas mixtures more transport phenomena can be studied. We can write down the following two phenomenological equations for the heat flux q as well as for the

particle flux $\underline{j}_\ell$ caused by a temperature or concentration gradient

$$\underline{q} = -\lambda \quad \underline{\nabla}T - \frac{p}{x_A x_B} \mathscr{D}_T \underline{\nabla} x_\ell \tag{12}$$

$$\underline{j}_\ell = -\frac{n}{T} D_T \underline{\nabla}T - n \quad D \quad \underline{\nabla} x_\ell \tag{13}$$

where p is the pressure of the gas, x_ℓ the mole fraction of component ℓ (ℓ = A or B), n the particle density and T the temperature. The first term of Eq. (12) reflects the ordinary heat conduction, and the last term of Eq. (13) diffusion. The two remaining terms correspond to cross effects: a temperature gradient also gives rise to a particle flux (thermal diffusion; D_T is the thermal diffusion coefficient). Inversely, a concentration gradient gives rise to a heat flux (diffusion thermo effect or Dufour effect, the reciprocal effect of thermal diffusion; $\mathscr{D}_T$ is the diffusion-thermo coefficient). These two effects are convected by the Onsager relation

$$D_T = \mathscr{D}_T \ . \tag{14}$$

This relation was confirmed experimentally by Waldmann in 1946 [33].

When a magnetic field is applied the scalar transport coefficients in Eqs. (12) and (13) have to be replaced by second rank tensors (*cf.* Eq. (2a)):

$$\underline{q} = -\underline{\underline{\lambda}} \quad \cdot \underline{\nabla}T - \frac{p}{x_A x_B} \underline{\underline{\mathscr{D}}}_T \cdot \underline{\nabla} x_\ell \tag{15}$$

$$\underline{j}_\ell = -\frac{n}{T} \underline{\underline{D}}_T \cdot \underline{\nabla}T - n \quad \underline{\underline{D}} \cdot \underline{\nabla} x_\ell \tag{16}$$

where for $\underline{\underline{\lambda}}$, $\underline{\underline{\mathscr{D}}}_T$, $\underline{\underline{D}}_T$ and $\underline{\underline{D}}$ one has schemes similar to that for $\underline{\underline{\lambda}}$ in Eq. (2b)

$$\underline{\underline{T}} = \begin{pmatrix} T^{\perp} & -T^{tr} & 0 \\ T^{tr} & T^{\perp} & 0 \\ 0 & 0 & T^{/\!/} \end{pmatrix} \qquad (T = \lambda, \mathscr{D}_T, D_T \text{ or } D). \tag{17}$$

The diagonal elements of these matrices are even, the off-diagonal ones are odd in the magnetic field:

$$\begin{aligned} T^{//}(B) &= T^{//}(-B) \\ T^{\perp}(B) &= T^{\perp}(-B) \\ T^{tr}(B) &= -T^{tr}(-B) \end{aligned} \qquad (T = \lambda, \mathscr{D}_T, D_T \text{ or } D). \tag{18}$$

Onsager relations in the presence of a magnetic field require that

$$\mathscr{D}_{T_{ij}}(B) = D_{T_{ji}}(-B) \tag{19}$$

or, combining the Eqs. (18) and (19)

$$\left.\begin{aligned} \mathscr{D}_T^{//}(B) &= D_T^{//}(-B) = D_T^{//}(B) \\ \mathscr{D}_T^{\perp}(B) &= D_T^{\perp}(-B) = D_T^{\perp}(B) \\ \mathscr{D}_T^{tr}(B) &= -D_T^{tr}(-B) = D_T^{tr}(B) \end{aligned}\right\} \quad \underline{\underline{\mathscr{D}}}_T(B) = \underline{\underline{D}}_T(B). \tag{20}$$

In the same way as for the coefficients of $\underline{\underline{\lambda}}$, theoretical expressions for the field dependence of the coefficients of $\underline{\underline{\mathscr{D}}}_T$, $\underline{\underline{D}}_T$ and $\underline{\underline{D}}$ have been derived[30,31]: equations similar to Eqs. (6), (7) and (8) are found with $\Psi^{\mathscr{D}_T}$, Ψ^{D_T} or Ψ^{D} replacing Ψ^{λ}. From these expressions an interrelation between the various transverse coefficients follows

$$|D_T^{tr}| = \sqrt{x_1 x_2 \, D^{tr} \frac{\lambda^{tr}}{n\,k}} \quad . \tag{21}$$

This relation is only valid for the contribution of each polarization separately.

From early measurements of the field effect on thermal conductivity (see Fig. 1) it followed, that data on at least two elements of $\underline{\underline{\lambda}}$ (*e.g.*, $\lambda^{//}$ and $\lambda^{\perp}$) are needed to determine the relative importance of the various polarizations. The interest in measuring now also the field effects on the other transport properties, by measuring, *e.g.*, two coefficients of each tensor $\underline{\underline{\mathscr{D}}}_T$, $\underline{\underline{D}}_T$ and $\underline{\underline{D}}$, lies in the following three facts. First of all these measurements give analogous information as the measurements of $\underline{\underline{\lambda}}$, namely information on the presence of various polarizations in heat conducting and diffusing gases: $\Psi^{\mathscr{D}_T}_{12}$, $\Psi^{D_T}_{12}$, Ψ^{D}_{12}, $\Psi^{\mathscr{D}_T}_{11}$, $\Psi^{D_T}_{11}$ and Ψ^{D}_{11} are determined. These Ψ's are related by kinetic theory to collision integrals or effective cross sections, which are strongly dependent on the nonspherical part of the intermolecular potential. Since all coefficients are described by the same τ_{12} and τ_{11} a check on the reliability of the results is obtained. Secondly an Onsager reciprocity rela-

tion in the presence of a magnetic field is tested (Eq. (20)). Thirdly the validity of the interrelation between the different effects (Eq. (21)) can be checked.

III. EXPERIMENTAL

Perhaps one of the most interesting features of the Senftleben-Beenakker effect is the existence of *transverse effects*, *i.e.*, transport perpendicular to both applied gradient and magnetic field. Since the apparatus for measuring the parallel and perpendicular coefficients are in principle the same as those used for measuring transport coefficients in the field free case, we will only describe the apparatus for measuring transverse coefficients. The transverse effects caused by a temperature gradient or concentration gradient (*cf.* Eqs. (15) and (16)) are illustrated in Fig. 3. For the thermal conductivity "transverse effect" means that under the influence of a magnetic field a transverse heat transport will occur perpendicular to the applied temperature gradient (Fig. 3a). In the same way transverse particle flux perpendicular to the applied concentration gradient will occur in the case of diffusion (Fig. 3d). For the

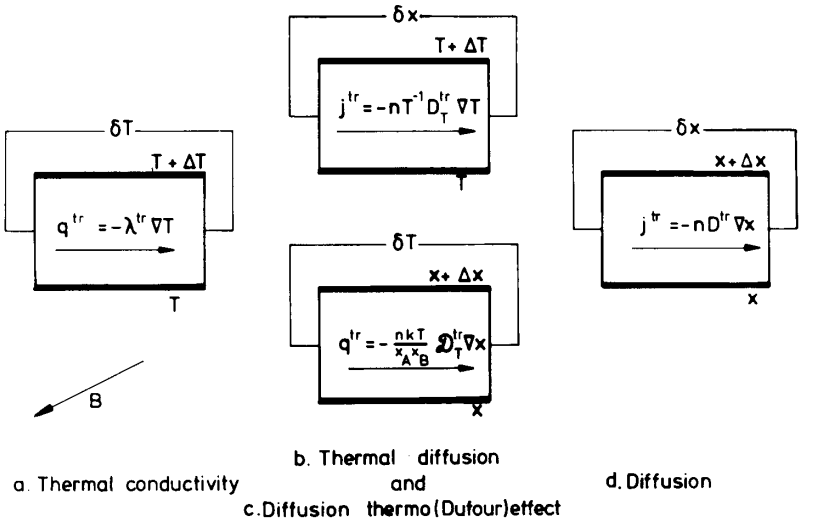

Fig. 3. The physical meaning of the transverse effects caused by a temperature gradient or concentration gradient in a magnetic field perpendicular to the plane of the drawing.

cross effects thermal diffusion and diffusion thermo-effect one gets a transverse particle flux perpendicular to the applied temperature gradient and a transverse heat flux perpendicular to the applied concentration gradient, respectively (Figs. 3b and 3c). Before going into the details of each apparatus separately given in Figs. 4 through 8, we will discuss some general features.

In principle each apparatus for measuring these effects consists of a rectangular or cylindrical channel. The directions of magnetic field, applied gradient and transverse flux will be the same in each experiment (see Fig. 3). Furthermore the dimension of the channel in the direction of the applied gradient will be called height (h), in the direction of the transverse flow width (w) and in the direction of the applied field depth (d). These dimensions are listed together with some other data in Table II.

Rather than measuring directly the transverse heat flux $\underline{q}^{tr}$ (or particle flux j^{tr}), a corresponding temperature difference δT (concentration difference δx) across the width of the channel is measured, because this is experimentally much simpler. For the heat conductivity experiment, *e.g.*, in the stationary case the observed temperature difference δT across the width w of the channel is found to be using Eq. (2)

$$\delta T = \frac{w}{h} \frac{\lambda^{tr}}{\lambda} \Delta T \tag{22}$$

where ΔT is the applied temperature difference across the height h of the channel ($\nabla T = \Delta T/h$). As will be clear from Eq. (22), one should like to choose the ratio w/h as large as possible in order to achieve maximum sensitivity. However, in order to reduce the short-circuiting effect caused by the ends of the channel, which are kept at temperatures T and $T + \Delta T$ one would like to have $w/h \ll 1$. Consequently we will have to make a compromise and the height will be of the same order of magnitude as the width. Similar considerations hold for the diffusion experiment. Only in the case of a cross effect, when the transverse flux and the applied gradient have a different nature the sensitivity can be increased dramatically by choosing $w/h \gg 1$. For the thermal diffusion, *e.g.*, one has

$$\delta x = \frac{w}{h} \frac{D_T^{tr}}{D} \frac{\Delta T}{T} \quad . \tag{23}$$

When temperature differences are measured (λ^{tr} and $\mathcal{D}_T^{tr}$), the walls are made of thin, low thermal conductance material (Mylar). When concentration differences are measured (D_T^{tr} and D^{tr}) brass is used to ensure temperature homogeneity.

The particular features of each apparatus will now be discussed separately.

Table II

Some data from the various apparatus described in this section. Note that w is the dimension of the channel in the direction of the transverse flow and h in the direction of the applied gradient. The data for "driving force", "effect" and "sensitivity" are only meant as a rough indication.

Experiment	Year	Channel material	Channel dimensions			Ratio	Driving force		Effect		Sensitivity		Ref.
			w (mm)	h (mm)	d (mm)	$\frac{w}{h}$	ΔT (K)	Δx_{max}	δT_{max} (K)	δx_{max}	δT_{min} (K)	δx_{min}	
λ^{tr}	1967	mylar	23*)	45	23*)	0.51	15		5×10^{-4}		2×10^{-5}		7
D_T^{tr}	1974	brass	1480	6	6	247	10			2×10^{-4}		2×10^{-6}	13**)
$\mathscr{D}_T^{tr}$	1977	mylar	10	80	1	0.13		0.2	2×10^{-4}		1×10^{-5}		14
D^{tr}	1978	brass	20	60	0.7	0.33		0.4		2×10^{-5}		2×10^{-7}	16

*) Cylindrical

**) The very first experiments were performed in an apparatus with w = 2250 mm, see Ref. 34.

a. Thermal conductivity: λ^{tr}. A schematic diagram of the apparatus is given in Fig. 4. The cylindrical wall was constructed from a Mylar sheet of thickness 190 μm, while upper and lower plate were made of brass. A temperature gradient was set up by an electric heater in the top plate. The field induced transverse temperature difference is measured directly in a Wheatstone bridge arrangement with two small thermistors glued at both sides of the channel.

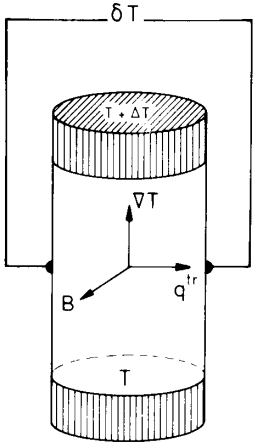

Fig. 4. Schematic diagram of the thermal conductivity apparatus. The direction of the transverse heat flux is the one observed for N_2.

b. Thermal diffusion: D_T^{tr}. In the case of the thermal diffusion experiment, we have a transverse concentration difference due to an applied temperature difference. A very high sensitivity can be achieved by an appropriate choice of the geometry ($w/h >> 1$). In order to fit such a channel between the poles of the magnet a design as shown in Fig. 5b is chosen. The channel consists of 20 sections connected by holes. This yields a channel of effective width 1480 mm. Adjacent channel sections are separated by means of brass foil of 50 μm thickness. The concentration difference across the channel is determined by measuring the difference in thermal conductivity of the gas at both ends of the channel. For this purpose the ends of the channel were connected to two chambers in a thermally isolated copper block (not shown in Fig. 5 and placed outside the magnetic field) in which two thermistors (katharometer type) were placed. By heating up these thermistors in a Wheatstone bridge arrangement very small changes of the thermal conductivity (and thus very small corresponding concentration differences; see Table II) could be detected. Calibration was achieved using mixtures of known composition.

c. Diffusion thermo (Dufour) effect: $\mathcal{D}_T^{tr}$. An apparatus previously used for another experiment[12] was employed. The schematic diagram of this apparatus in Fig. 6 shows the rectangular channel made of Mylar of thickness 75 μm. A concentration gradient across the length of the channel is set up by connecting each end of the channel to a 20 ℓ bulb filled with a pure component

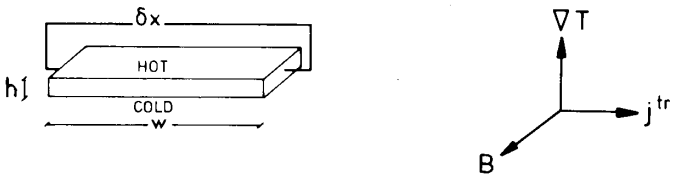

5a

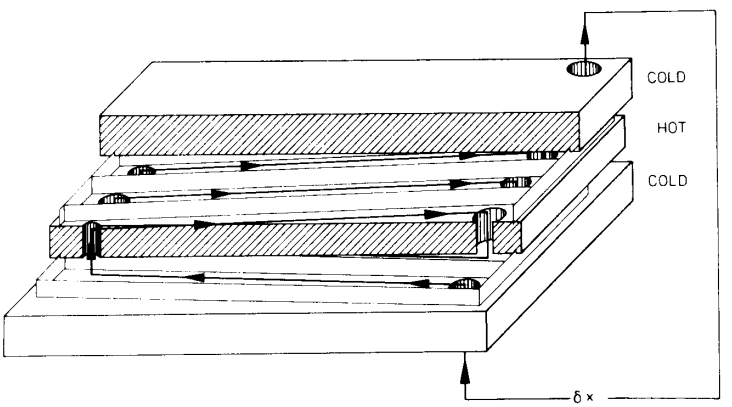

5b

Fig. 5a.Schematic diagram of the thermal diffusion apparatus. The direction of the particle flux is the one observed for N_2 in a N_2-Ar mixture.

Fig. 5b.Thermal diffusion apparatus used to fit the channel between the poles of the magnet. Compare with Fig. 5a and note that h is the dimension of the channel in the direction of the applied gradient and w is the direction of the transverse flux. In order to obtain a high sensitivity w/h has been chosen as high as 247.

allowing measuring times of several hours. This decreasing concentration gradient is monitored by measuring the difference in thermal conductivity between the gas mixtures directly at the ends of the channel. The field induced transverse heat flux q^{tr} gives rise to a temperature difference δT across the width of the channel which is measured by means of two small thermistors glued onto the narrow walls of the channel. In order to relate the observed temperature difference to q^{tr}, a calibration heat flux was produced by electrically heating one side of the channel.

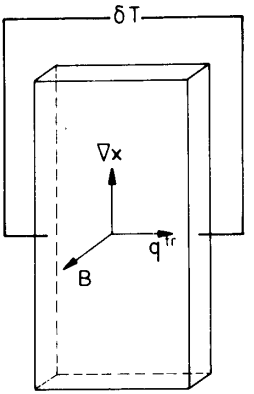

Fig. 6. Schematic diagram of the diffusion thermo apparatus. The directions of the applied N_2 concentration gradient and of the observed heat flux for a N_2-Ar mixture are indicated.

d. Diffusion D^{tr}. The apparatus is shown in Fig. 7. The concentration gradient is set up by connecting each end of the channel to a 50 ℓ bulb. The measurement of the transverse concentration difference is done in the same way as for the thermal diffusion experiment: two small holes in the narrow walls of the channel are connected to two detection chambers in a copper block placed outside the magnetic field.

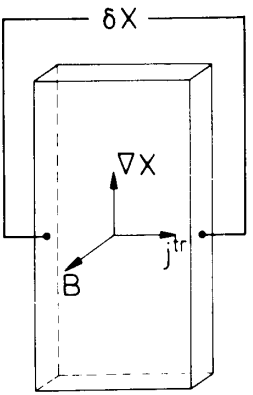

Fig. 7. Schematic diagram of the diffusion apparatus. The indicated directions of applied concentration gradient and of the observed transverse particle flux are those for N_2 in a N_2-Ar mixture.

IV. RESULTS AND DISCUSSION

First of all consistency tests have been performed with each apparatus. It was verified that the measured transverse fluxes are linear in the applied gradients and that no effects were observed for noble gases. Furthermore it was checked that the transverse effects are odd functions of the magnetic field. Since the directions of the transverse fluxes are determined by the sign of the molecular g-factor[10], it could also be verified that the observed directions of the transverse fluxes are in agreement with the signs of the molecular g-factors obtained from other experiments. In some cases previously unknown signs of g-factors were determined.

Experimental results for the gas mixture N_2-Ar ($x_{N_2} = 0.5$; T = 300 K) for each experiment, corrected for (small) Knudsen effects, are shown in the Figs. 8a through 8d as an example of all the results obtained. Note that λ^{tr} could not be measured at 300 K for experimental reasons (radiative heat losses). However, this curve was constructed from the $\Delta\lambda^{\perp}$ and $\Delta\lambda^{/\!/}$ data, which can be reliably done, as was shown from the 85 K data where all three curves were measured (see Fig. 2).

It should be remarked that also the difference between the perpendicular and parallel coefficients can be measured in principle in the same four apparatus described in Figs. 4 through 7 by appropriately orienting the magnetic field with respect to the apparatus. In this way $D_T^{/\!/} - D_T^{\perp}$ and $\mathscr{D}^{/\!/} - \mathscr{D}^{\perp}$ were measured (see Figs. 8b and 8d). It was verified that these effects are even in the field.

By comparing the results of thermal diffusion and diffusion thermo-effect (Figs. 8b and 8c) the Onsager relation expressed in the third line of Eq. (20) can be verified. The two coefficients D_T^{tr} and $\mathscr{D}_T^{tr}$ are found to agree within the joint experimental error, which indeed confirms an Onsager reciprocity relation in the presence of a magnetic field.

The observed field dependence of the Senftleben-Beenakker effects is in excellent agreement with the theoretical predictions of kinetic theory[35,36,25,29] based on the solution of the linearized Waldmann-Snider equation. A detailed account of the theory is outside the scope of the present survey. The results of a comparison between experimental results and theory will be treated summarily. Furthermore it was found that the four experiments (λ, D_T, $\mathscr{D}_T$ and D) yield the same values for τ_{12} and τ_{11} in agreement with theory (see Eqs. (6) - (8)).

In the kinetic theory, starting from the Waldmann-Snider equation, *i.e.*, the quantum mechanical analogon of the Boltzmann equation, one finds expressions for τ and Ψ in terms of collision integrals or, equivalently, effective cross sections. For $\tau_{\alpha\beta}$ one has

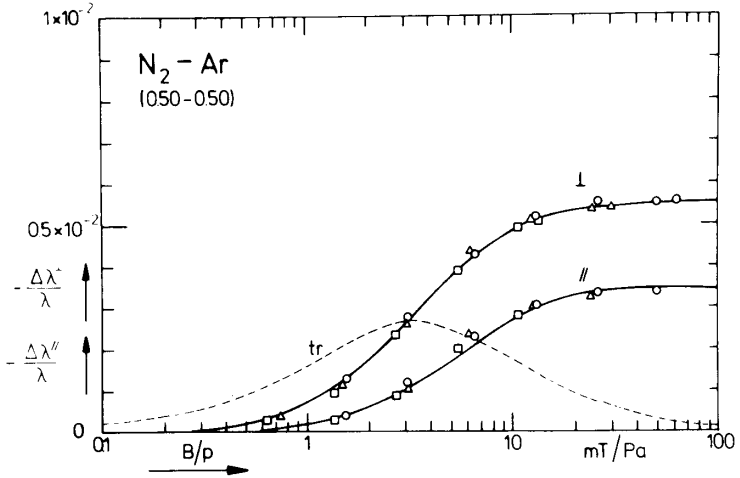

Fig. 8a. Experimental results for the thermal conductivity coefficients $\Delta\lambda^{\perp}/\lambda$ and $\Delta\lambda^{/\!/}/\lambda$ for N_2-Ar at T = 300 K. The drawn curves are the theoretical curves fitted to the experimental points. The dashed curve reflects the behavior of λ^{tr}/λ as calculated with the data obtained from the other two coefficients. Different symbols denote different pressure runs ranging from 20 Pa to 250 Pa.

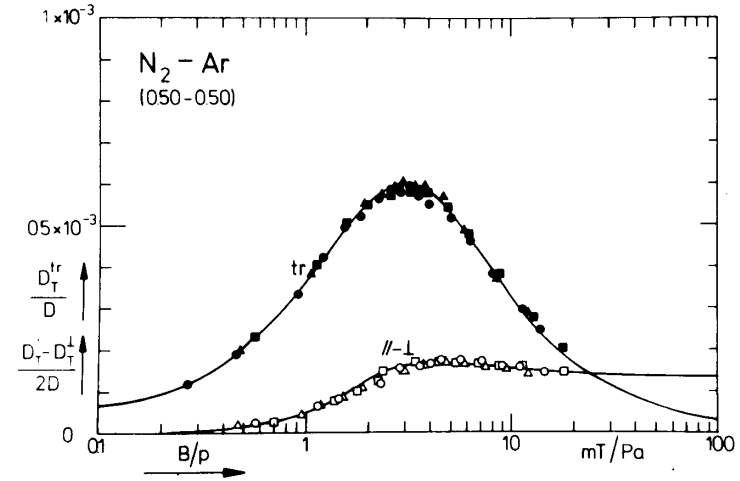

Fig. 8b. Experimental results for the thermal diffusion coefficients D_T^{tr}/D and $(D_T^{/\!/} - D_T^{\perp})/2D$ for N_2-Ar at T = 300 K. The drawn curves are the theoretical curves fitted to the experimental points. Different symbols denote different pressure runs ranging from 100 Pa to 250 Pa.

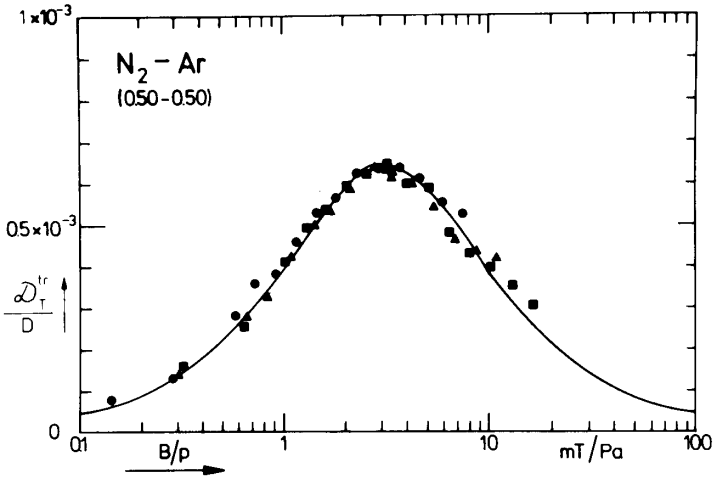

Fig. 8c.Experimental results for the transverse diffusion thermo (Dufour) coefficient for N_2-Ar at 300 K. The drawn curve is the theoretical curve fitted to the experimental points. Within the joint experimental error the results for $\mathcal{D}_T^{tr}/D$ coincide with the ones for D_T^{tr}/D (compare Figs. 8b and 8c). Different symbols denote different pressure runs ranging from 100 Pa to 250 Pa.

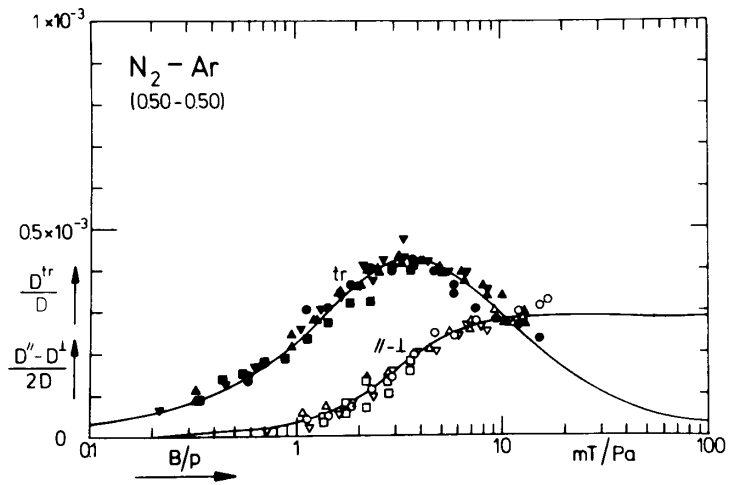

Fig. 8d.Experimental results for the diffusion coefficients D^{tr}/D and $(D^{//} - D^{\perp})/2D$ for N_2-Ar at 300 K. The drawn curves are the theoretical curves fitted to the experimental points. Different symbols denote different pressure runs ranging from 150 Pa to 600 Pa.

$$\tau_{\alpha\beta}^{-1} = n\, v\, \mathcal{S}_{\alpha\beta} , \qquad \alpha\beta = 12 \text{ or } 11 \tag{24}$$

where n is the particle density, v is the average relative velocity. The effective cross section $\mathcal{S}_{\alpha\beta}$ is defined as, *e.g.*,

$$\mathcal{S}_{11} = \langle \underline{W}\ \underline{J} : \mathcal{R}\ \underline{J}\ \underline{W} \rangle\ v^{-1} \tag{25}$$

with $\mathcal{R}$ the collision operator of the Waldmann-Snider equation. Physically, $\tau_{\alpha\beta}$ or $\mathcal{S}_{\alpha\beta}$ describe the decay through collisions of the angular momentum dependent polarization of type $\alpha\beta$. The quantities $\Psi_{\alpha\beta}$, which determine the magnitude of the field induced change in the transport properties (Eqs. (6) - (8)), have the form, *e.g.*,

$$\Psi_{11}^{\lambda} = \frac{\mathcal{S}^2 (q \leftrightarrow W\ J)}{\mathcal{S}_q \mathcal{S}_{11}} . \tag{26}$$

Physically, $\mathcal{S}(q \leftrightarrow W\ J)$ is the coupling cross section which describes the production of the W J polarization from the heat flow q through collisions. $\mathcal{S}_q$ is the decay cross section for heat transport, which can be determined from the field free thermal conductivity coefficient $\lambda(0)$. Combining results for τ, Ψ and λ allows one to determine the cross sections separately. For mixtures the situation is considerably complicated by the fact that many more cross sections occur due to the presence of two species, but again the experimental results can be given in terms of cross sections.

In Table III the systems are given for which data have been obtained for λ, D_T, $\mathcal{D}_T$ and D. Some general conclusions concerning the cross sections will now be given.

- Production cross sections are always at least an order of magnitude smaller than the decay cross sections, the latter usually being of the order of the gas-kinetic cross sections. This is connected to the fact that these production cross sections are directly determined by the nonspherical part of the intermolecular potential.
- In some cases, the cross sections could be compared with cross sections from experiments on entirely different physical quantities: NMR, Depolarized Rayleigh Scattering, acoustical relaxation and the viscomagnetic effect. These results constitute a further verification of the kinetic theory for molecules with internal degrees of freedom.
- The fact that there is a contribution from the odd-in-J polarization W J (*i.e.*, $\Psi_{11} \neq 0$) can be shown to imply that the collision operator $\mathcal{R}$ is not self-adjoint.
- The cross sections provided by the experiment can be used to determine the intermolecular potential. Calculations have

Table III
The systems studied experimentally

Exp.	Heat conductivity			Thermal diffusion		Dufour effect	Diffusion	
Gas	$\frac{\lambda^{tr}}{\lambda}$	$\frac{\Delta\lambda^{\perp}}{\lambda}$	$\frac{\Delta\lambda^{/\!/}}{\lambda}$	$\frac{D_T^{tr}}{2D}$	$\frac{D_T^{/\!/}-D_T^{\perp}}{2D}$	$\frac{\mathcal{D}_T^{tr}}{D}$	$\frac{D^{tr}}{D}$	$\frac{D^{/\!/}-D^{\perp}}{2D}$
nH_2	26K-110K	300K	300K					
nH_2-He				300K	300K			
nH_2-Ne				300K	300K			
nH_2-Ar				300K	300K			
pH_2	86K-110K	300K	300K					
pH_2-Ar				300K	300K			
HD	22K-85K	38K-300K	38K-300K					
HD-He		85K, 300K	85K, 300K	300K	300K			
HD-Ne		85K, 300K	85K, 300K	300K	300K			
HD-Ar		85K, 300K	85K, 300K	300K	300K			
nD_2	26K, 85K	300K	300K					
nD_2-He				300K	300K			
nD_2-Ne				300K	300K			
nD_2-Ar				300K	300K			
oD_2	85K	300K	300K					
N_2	85K	82K-300K	82K-300K					
N_2-He		85K, 300K	85K, 300K	300K	300K		300K	300K
N_2-Ne		85K, 300K	85K, 300K	300K	300K			
N_2-Ar		85K, 300K	85K, 300K	300K	300K	300K	300K	300K
O_2	85K	300K						
HCl		300K						
DCl		300K						
HCN		300K						
CO	85K	82K-300K						
CO_2		300K						
OCS		300K						
NO	85K							
CH_4	85K	82K-300K	82K-300K					
CD_4	85K	82K-300K	82K-300K					
CF_4	93K	300K	300K					
CH_3CN		300K	300K					
CH_3F		300K	300K					
CD_3F		300K	300K					
CHF_3		300K	300K					
CDF_3		300K	300K					
NH_3		300K	300K					
ND_3		300K	300K					
SF_6		300K	300K					
Ref.	6,7,8,9,10,11			12,13		14,15	16	

been performed starting from an assumed (angle-dependent) potential model. Models using rigid ellipsoids cannot explain the experimental results, as should be expected. Quantum mechanical calculations have been performed only for relatively simple cases, *e.g.*, H_2-He, in which a number of cross sections have been calculated[37,38].
Finally, after complete analysis of the results of each experiment separately (measurements on the diffusion coefficients are still in course), one will be able to compare the results using the interrelation (21) as a further check on the theory.

REFERENCES

1. J. Korving, H. Hulsman, G. Scoles, H.F.P. Knaap, and J.J.M. Beenakker, Physica 36, 177 (1967).
2. H. Hulsman, F.G. van Kuik, K.W. Walstra, H.F.P. Knaap, and J.J.M. Beenakker, Physica 57, 501 (1972).
3. A.L.J. Burgmans, P.G. van Ditzhuyzen, H.F.P. Knaap, and J.J.M. Beenakker, Z. Naturforsch. 28a, 835 (1973).
4. A.L.J. Burgmans, P.G. van Ditzhuyzen, and H.F.P. Knaap, Z. Naturforsch. 28a, 849 (1973).
5. P.G. van Ditzhuyzen, B.J. Thijsse, L.K. van der Meij, L.J.F. Hermans, and H.F.P. Knaap, Physica 88A, 53 (1977).
6. L.J.F. Hermans, P.H. Fortuin, H.F.P. Knaap, and J.J.M. Beenakker, Phys. Lett. 25A, 81 (1967).
7. L.J.F. Hermans, A. Schutte, H.F.P. Knaap, and J.J.M. Beenakker, Physica 46, 491 (1970).
8. L.J.F. Hermans, J.M. Koks, A.F. Hengeveld, and H.F.P. Knaap, Physica 50, 410 (1970).
9. J.P.J. Heemskerk, F.G. van Kuik, H.F.P. Knaap, and J.J.M. Beenakker, Physica 71, 484 (1974).
10. J.P.J. Heemskerk, G.F. Bulsing, and H.F.P. Knaap, Physica 71, 515 (1974).
11. B.J. Thijsse, W.A.P. Denissen, L.J.F. Hermans, H.F.P. Knaap, and J.J.M. Beenakker, Physica (1979), to be published.
12. G.E.J. Eggermont, P.W. Hermans, L.J.F. Hermans, and J.J.M. Beenakker, Phys. Lett. 57A, 29 (1976).
13. G.W. 't Hooft, E. Mazur, J.M. Bienfait, L.J.F. Hermans, H.F.P. Knaap, and J.J.M. Beenakker, Physica (1979), to be published.
14. E. Mazur, G.W. 't Hooft, and L.J.F. Hermans, Phys. Lett. 64A, 35 (1977).
15. E. Mazur, G.W. 't Hooft, L.J.F. Hermans, and H.F.P. Knaap, Physica (1979), to be published.
16. E. Mazur et al., Physica (1979), to be published.

17. A.C. Levi, G. Scoles, and F. Tommasini, Z. Naturforsch. 25a, 1213 (1970).
18. F. Tommasini, A.C. Levi, G. Scoles, J.J. de Groot, J.W. van den Broeke, C.J.N. van den Meijdenberg, and J.J.M. Beenakker, Physica 49, 299 (1970).
19. F. Tommasini, A.C. Levi, and G. Scoles, Z. Naturforsch. 26a, 1098 (1971).
20. V.D. Borman, L.L. Gorelik, B.I. Nikolaev, V.V. Sinitsyn, and V.I. Troyan, Sov.Phys.JETP 29, 959 (1969).
21. J.J. de Groot, J.W. van den Broeke, H.J. Martinius, C.J.N. van den Meijdenberg, and J.J.M. Beenakker, Physica 56, 388 (1971).
22. V.D. Borman, B.I. Nikolaev, and V.I. Troyan, Inzh.Fiz.Zh. (J.Eng.Phys.) 27, 640 (1974).
23. V.D. Borman, B.I. Nikolaev, and V.A. Chuzhinov, Sov.Phys. JETP 33, 881 (1971).
24. J.J.M. Beenakker and F.R. McCourt, Annu.Rev.Phys.Chem. 21, 47 (1970).
25. J.A.R. Coope and R.F. Snider, J.Chem.Phys. 56, 2056 (1972); ibid. 57, 4266 (1972).
26. J.J.M. Beenakker, H.F.P. Knaap, and B.C. Sanctuary, AIP Conference Proc. 11, 21 (1973).
27. J.J.M. Beenakker, Lecture Notes in Physics 31 (Springer-Verlag, Berlin), 413 (1974).
28. R.F. Snider, Lecture Notes in Physics 31 (Springer-Verlag, Berlin), 469 (1974).
29. H. Moraal, Phys.Rep. 17C, 225 (1975).
30. G.E.J. Eggermont, H. Vestner, and H.F.P. Knaap, Physica 82A, 23 (1976).
31. F.R. McCourt and R.F. Snider, J.Chem.Phys. 46, 2387 (1967).
32. H.F.P. Knaap and J.J.M. Beenakker, Physica 33, 643 (1967).
33. L. Waldmann, J.Phys.Rad. 7, 129 (1946); Z. Naturforsch. 4a, 105 (1949).
34. G.E.J. Eggermont, P. Oudeman, and L.J.F. Hermans, Phys. Lett. 50A, 173 (1974).
35. L. Waldmann. Z. Naturforsch. 12a, 660 (1957).
36. Yu.V. Mikhailova and L.A. Maksimov, Sov.Phys.JETP 24, 1265 (1967).
37. R. Shafer and R.G. Gordon, J.Chem.Phys. 58, 5422 (1973).
38. W.K. Liu and F.R. McCourt, Chem.Phys. 27, 281 (1978).